VOL. 11, NO. 8, APRIL 2016 ISSN 1819-6608
ARPN Journal of Engineering and Applied Sciences

www.arpnjournals.com

AMPLIFICATION EFFECT ON STRESS INTENSITY FACTOR AT DIFFERENT CRACK INTERVAL IN CORTICAL BONE

Noor Alia Md Zain[1], Ruslizam Daud[2], Khairul Salleh Basaruddin[2] and Wan Zuki Azman Wan Mohamad[1]
[1]Institute of Engineering Mathematics, Pauh Putra Campus, Universiti Malaysia Perlis, Arau, Perlis, Malaysia
[2]Fracture and Damage Mechanic Research Group, School of Mechatronic Engineering, Pauh Putra Campus, Universiti Malaysia Perlis, Arau, Perlis, Malaysia
E-Mail: aliazain@unimap.edu.my

ABSTRACT

Cortical bone fracture that caused by stress amplification effect is hypothesized to initiate and amplify by the existence of co-planar macro and micro cracks interaction. The amplified crack interactions within the human cortical bone are quite complicated to investigate because of the bone microstructure. At the microstructure level of bone, it is clear that every particle of the bone is essential in protecting the bone from fracturing. This paper aims to investigate the stress amplification effect of the stress intensity factor (SIF), K based on stress singularity located at the crack tips. Finite element models of two coplanar edge cracks for different crack distance s and crack interval b are developed based continuum mechanics theory and linear elastic fracture mechanics (LEFM) assumption. The SIF value accuracy is based on the developed singularity element around the crack tip. The result showed that the SIF of both coplanar cracks are exibit the different trend for Mode I and II. Moreover, the existence of crack interaction limit (CIL) and crack unification limit (CUL) have proved the theory of interacting cracks.

Keywords: stress intensity factor, crack interval, amplification effect.

INTRODUCTION

Human cortical bone which also known as compact bone plays a major role in daily human activities. Compact bone facilitates the main function of the bone which is to support the human body and cradle its soft organs (Marieb, 2007). Usually the bone fracture is determined by its mineral density and the age factor. However, there is a previous research which shows that decreasing bone mineral density is not the only factor that can lead to fracture mechanism (Doblaré, Garcıa, and Gómez, 2004). There are several parameters that can influence the fracture mechanism. One of the main functions of human cortical bone is to weight-bearing and absorbs shock of human body. Unfortunately in vitro studies the load conditions are different from the actual physiological loading (Chen, Tang, and Ju, 2001). This condition has caused the formation of microcracks in cortical bone. In this case, the behavior interaction between cracks is highly important. Hence, finite element method can be used to investigate the biomechanical behavior of the cortical bone with cracks.

There are three parameters which are used to characterize the stress which cause a component to fracture. These include the stress intensity factor (SIF) or K, elastic energy release rate,G and J-Integral, J. SIF is the stress field that surrounds the crack tip of an isotropic linear elastic material. The stress can be formulated as

$$\lim_{r\to 0}\sigma = \frac{K}{\sqrt{2\pi r}} f(\theta) \tag{1}$$

where K is the stress intensity factor but this equation is only valid near the crack tip. The $\frac{1}{\sqrt{r}}$ represents the stress field around the crack. Thus, the value of K determines the level of stress magnitude around the crack tip which has been done by previous researcher (Rudraraju, 2004). The value of K should not exceed the value of the critical crack intensity factor (K_c) because if the value of K is bigger than K_c, the material will fracture (Huang *et al.*, 2012).

Bone fracture can be intiated by single cracking and multiple cracking mechanisms. Multiple cracks interaction can be categorized into stress shielding and stress amplification. The complexity of interaction depends on the geometrical features, material properties and loading factor (Daud, 2013; Daud *et al.*, 2015). In bone fracture, study on stress shielding and stress amplification in cracking bones is growing in research. This study aims to investigate the stress amplification effect on SIF for the case of two coplanar cracks in cortical bone.

Stress amplification modeling

Bone fracture is caused by continuous crack propagation where it can be classified into 3 modes: Mode I, Mode II and Mode III. For Mode I, the crack tip is open because of the forces acting on it. The forces are in the opposite direction. The crack propagates in both y-axis and z-axis. For Mode II crack tip deformation, the shear stresses occur within the same plane. The force is parallel to the crack surface. The crack slide over the x-axis. For Mode III, the shear stresses occur out of the plane. The crack surface will slide over with each other in the z-axis.

In human bone, cracks usually occur due to the repetitive or cyclic loading of force or large force acting on the bone rather abruptly. In clinical aspect, people usually undergo total hip replacement due to the damage in the femoral head of the femur bone. This is where the crack propagation usually occurs. The propagation of crack is dependent on human body posture. This is where

the modes of crack propagation are used. The position of the force will represent the human body posture. The crack propagation is strongly based on the stress intensity factor (K) of the bone and bone fracture resistance (Alia *et al.*, 2014). Human bone consists of a porous microstructure. Hence, the linear elastic fracture mechanics and the value of K determine the bone's resistance of crack propagation.

There are several methods that can be adopted to find the value of K. These include the singular element, enriched element, stress intensity function, remeshing technique, and also the boundary element method. Most of fracture mechanic problem has been widely solved by using finite element method which developed the standard displacement approximation by discontinuous fields through the partition of unity (Kumar *et al.*, 2015). The most likely method to be used is the singular element method where it is based on 8-node rectangular element used in meshing by connecting the mid-side nodes to the nearest node. The next step is to move the two midside nodes to the quarter point close to the singular point (Shah, Ferracane *et al*., 2009). The Jacobian method can help to capture the singularities. The singularity is determined by the apex of the crack found. If there are two different materials found in the singularity problem, there is no consideration of the elastic constant and local geometry of the material but the deformation mode must also be taken into account (Benbarek *et al*., 2013). This happens when there are different structures of bone tissues inside the bone which divided into the compact bone tissue and spongy bone tissue.

In calculating the value of SIF, at least two points around the crack tip should be selected to analyze it. There is a plastic zone around the crack tip which applies plastic deformation. Hence, linear elastic fracture mechanics is not valid in such an area. Based on previous research (Sanati *et al*., 2014), there are calculation of radius where the region of plastic zone takes place which located around the crack tips. It was attained by the following equations for plane stress and plane strain states, correspondingly:

$$r_p = \frac{1}{\pi}\left(\frac{K_I}{\sigma_y}\right)^2 \tag{2}$$

$$r_p = \frac{1}{3\pi}\left(\frac{K_I}{\sigma_y}\right)^2 \tag{3}$$

The crack failure in this research consist of Mode I and Mode II crack deformation. Hence, the investigation will focus on two different value of K which are K_I and K_{II}. The corresponding value of the stress field can be expressed into these two equation:

$$K_I = \lim_{r\to 0}\sqrt{2\pi r}\,\sigma_{yy}(r,0) \tag{4}$$

$$K_{II} = \lim_{r\to 0}\sqrt{2\pi r}\,\sigma_{xy}(r,0) \tag{5}$$

where σ represents the amount of stress acted on the crack tip depends on the direction of the force which clearly represents by Mode I and Mode II crack deformation. It can be expressed as:

$$\sigma_{ij} = \sigma_{ij}^{I} + \sigma_{ij}^{II} \tag{6}$$

Equation. (6) represents the amount of stress acted on the crack tip where *i* and *j* represent the direction of crack propagation. I and II represent the mode of crack deformation (Zain *et al*., 2014). Based on previous research done by Olvera, Zimmermann, and Ritchie (2012) shows that fracture toughness of human cortical bone in the transverse coordination actually decreases when mixed mode fracture is increasing. This specifies that resistance to fracture in this orientation is lower in mode II compared to mode I deformation.

There are many methods of computing the value of K. The most widely used method consists of conservation integrals where *J* integral is used to calculate the energy release rate for crack propagation. The other method is crack opening displacements at a crack tip. The distance between two crack tips, b which is known as crack interval can be analyzed to compute the value of K.

Based on previous research which was done by (Wen *et al.*, 2012), the value of stress intensity factor which is gained from the value of *b* can be written down in the following equation:

$$K_I = \frac{E}{8(1+\nu^2)}\sqrt{\frac{2\pi}{b}}\,\delta_2(\theta) \tag{7}$$

$$K_{II} = \frac{E}{8(1-\nu^2)}\sqrt{\frac{2\pi}{b}}\,[\delta_2(\theta)\cos\theta + \delta_3(\theta)\sin\theta] \tag{8}$$

where b, δ_1, δ_2, δ_3 are the relative displacements between the crack surfaces in the x , y , and z directions while E is the Young's modulus and ν is the Poisson' ratio of the cortical bone.

A finite element (FE) model of double edge crack has been constructed using ANSYS APDL 14 software. Figure-1 shows the meshing element, 8 nodes quadrilateral elements for double coplanar cracks. C_1 represent crack tip 1 while C_2 represents crack tip 2. Crack interval, b located at crack tip 2 remain to be constant at 14 mm while several value of b is chosen to analyze the relationship of b and stress intensity factor.

ARPN Journal of Engineering and Applied Sciences

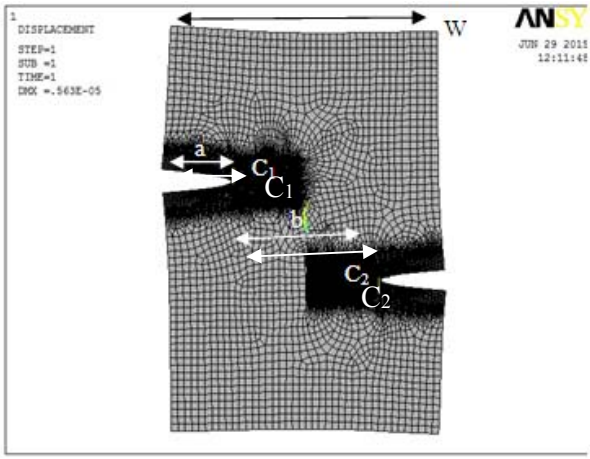

Figure-1. Finite element model of double coplanar edge cracks.

Five nodes of path network have been chosen in calculating the value of K_I and K_{II} at the crack tips. Displacement extrapolation method (DEM) has been employed in this modeling, where K_I and K_{II}expressed by:

$$K_I = \frac{E}{3(1+\nu)(1+\kappa)}\sqrt{\frac{2\pi}{L}}\left(4(v_2 - v_4) - \frac{(v_3 - v_5)}{2}\right) \quad (9)$$

$$K_{II} = \frac{E}{3(1+\nu)(1+\kappa)}\sqrt{\frac{2\pi}{L}}\left(4(u_2 - u_4) - \frac{(u_3 - u_5)}{2}\right) \quad (10)$$

where $\kappa = \frac{3-4\nu}{1-\nu}$ since plain strain are used (Xu and Li, 2012). L indicates the length of the specimen used while u_n, v_n are both displacement indisplacement in the internal Cartesian coordinate system

RESULTS AND DISCUSSIONS

Relationship between SIF, K and crack interval, b.

The SIF data values obtained from computational method are compared with analytical values which based on previous experimental research. The value of geometric stress intensity correction factor, Y were obtained from values of stress intensity factor, K where $K_o = \sigma\sqrt{\pi a}$. The Y formulation is (Woo and Kuruppu, 1982):

$$Y_I = \frac{K_I}{K_o} \quad (11)$$

$$Y_{II} = \frac{K_{II}}{K_o} \quad (12)$$

Table-1 and Table-2 show the associated geometry correction factor Y_I and Y_{II} for crack tip 1 and crack tip 2 at a range of crack interval, *b*. The width, w of the specimen is 60 mm. The crack length, *a* for crack tip 1 is chosen between 2 mm and 28 mm based on value of the crack interval, *b*.

Table-1. Value of geometric stress intensity correction factor for crack tip 1.

a (mm)	b (mm)	b/a	Y_I	Y_{II}
28	**18**	**0.64**	**2.65**	**0.13**
26	20	0.77	2.39	0.15
24	22	0.92	2.15	0.15
22	24	1.09	1.94	0.15
20	26	1.30	1.76	0.15
18	28	1.56	1.60	0.14
16	30	1.88	1.45	0.13
15	32	2.13	1.38	0.12
14	34	2.43	1.32	0.11
12	36	3.00	1.21	0.10
10	38	3.80	1.11	0.08
8	40	5.00	1.02	0.07
6	42	7.00	0.94	0.05
4	44	11.00	0.91	0.04
2	46	23.00	0.88	0.03

ARPN Journal of Engineering and Applied Sciences

Table-2. Value of geometric stress intensity correction factor for crack tip 2.

a (mm)	b (mm)	b/a	Y_I	Y_{II}
14	**18**	**1.28**	**0.53**	**0.33**
14	20	1.43	0.66	0.27
14	22	1.57	0.79	0.23
14	24	1.71	0.93	0.20
14	26	1.86	1.06	0.17
14	28	2.00	1.21	0.14
14	30	2.14	1.28	0.13
14	32	2.29	1.36	0.12
14	34	2.43	1.53	0.11
14	36	2.57	1.73	0.10
14	38	2.71	1.98	0.09
14	40	2.86	2.33	0.09
14	42	3.00	2.89	0.10
14	44	3.14	4.12	0.12
14	46	3.29	4.53	0.33

For crack tip 2, the *a* value has been fixed to 14 mm. Y_I indicates the of geometric stress intensity correction factor related to Mode I crack deformation while Y_{II} tends to propagates in Mode II. It can be seen that values for Y_I are higher compared to are higher compared to Y_{II} values. This is due to the model's major deformation is actually in Mode I but there is a slight effect in Mode II deformation where the force is acting perpendicularly within each crack in the double edge crack based on Figure-2. Hence, there is a small significance of K_{II} in the model simulated. In this research, the value of crack length, *a* indicates the changes in value of crack interval, *b*.

Values of geometric stress intensity correction factor in Table-2 specifies the K located at second crack tip where the crack length is fixed to 14 mm. There are difference in term of values between Y in crack tip 1 and crack tip 2. The Y in crack tip 2 have lower values compared to crack tip 2 at lower value of *b*. When the value of *b* increase, the *Y* value in crack tip 2 increase. Constrastingly in crack tip 1, as the value of *b* increase, the Y value drops to a minimum value. It can be seen more clearly in Figure-4 and Figure-5.

Comparison crack interaction factor with analytical data

Figure-2 indicates the comparison between numerical data; which is taken from the finite element model developed in ANSYS software and the analytical data. The SIF data is compared to analytical results of (Gross, Srawley, and Brown Jr, 1964) which can be expressed as:

$$K_I = \sigma\left(\sqrt{\pi a}\right)\left(1.12 - 0.23(a/w) + 10.6(a/w)^2 - 21.7(a/w)^3 + 30.4(a/w)^4\right) \quad (13)$$

The values of single crack and analytical crack are almost identical. There are two intersection points can be seen on the graph which indicates crack unification limit (CUL) and crack interaction limit (CIL). The patterns of the graph show that it has a unification limit at early stages of a/w where all the lines in the graph converge with each other at a/w = 0.47. The second intersection point reflects the CIL where a/w = 0.33.

This graph shows that the values of crack interaction factor are almost similar between values of the analytical result or theoretical results based on Brown and Srawley's (1966) theory. This has shown that the numerical results obtained from the finite element simulation have been verified.

Figure-2 also indicates the comparison between numerical data and analytical data. Equation. (13) is used for comparison. The same equation is used by Gross *et al.*, (1964). The values of single crack and analytical crack are almost identical. There are two intersection points can be seen on the graph which indicates crack unification limit (CUL); which indicates the starting point of strong interaction region and crack interaction limit (CIL); which indicates the maximum interaction limit occur at the crack tip. The patterns of the graph show that it has a unification limit at early stages of a/w where all the lines in the graph converge with each other at a/w = 0.33.The second intersection point reflects the CIL where a/w = 0.47. This graph shows that the value of crack interaction factor are almost similar between values of the analytical result or theoretical results based on Brown and& Srawley's (1966)

theory. This has shown that the numerical results obtained from the finite element simulation have been verified.

Figure-3 shows the K_I and K_{II} in double edge crack for crack tip 2 while Figure-4 displays the K_I and K_{II} in double edge crack for crack tip 1. It can be seen that the value of K_I is much bigger compared to K_{II} because the crack deformation tends to grow in Mode I. There is only a minimum value of deformation occur in Mode II. The value of K decrease as the b/a increase in crack tip 2 while it is a vice versa for crack tip 2. The crack length, *a* was remain constant at crack tip 2. Hence, when the value of *a* in crack tip 1 is higher than the value of *a* in crack tip 2, the *Y* will give higher value in crack tip 1. The value of Y in crack tip 1 keeps on dropping until *a* in both crack tip are similar to each other. It can be seen in Figure 5 where the value of *Y* is similar at *b* = 32 where the specimen are stable at this point. The load acted on the specimen are equally distributed between crack tip 1 and crack tip 2.

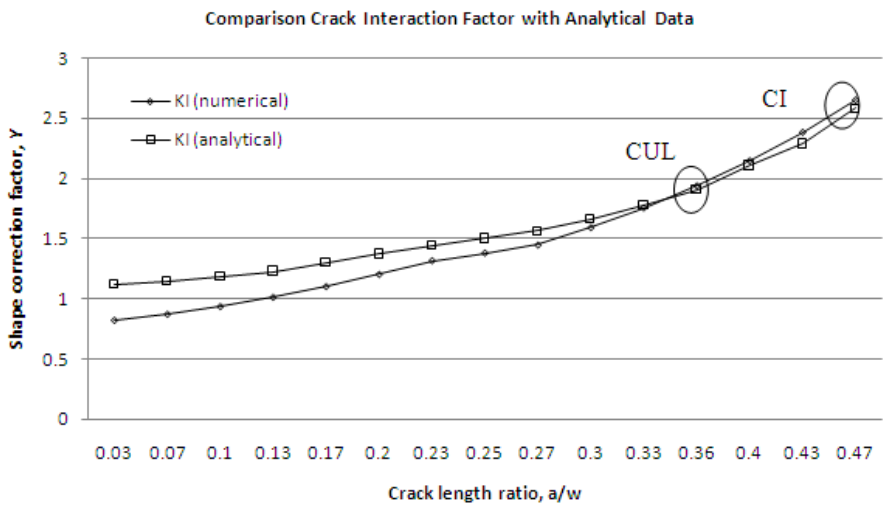

Figure-2. Comparison crack interaction factor with analytical data.

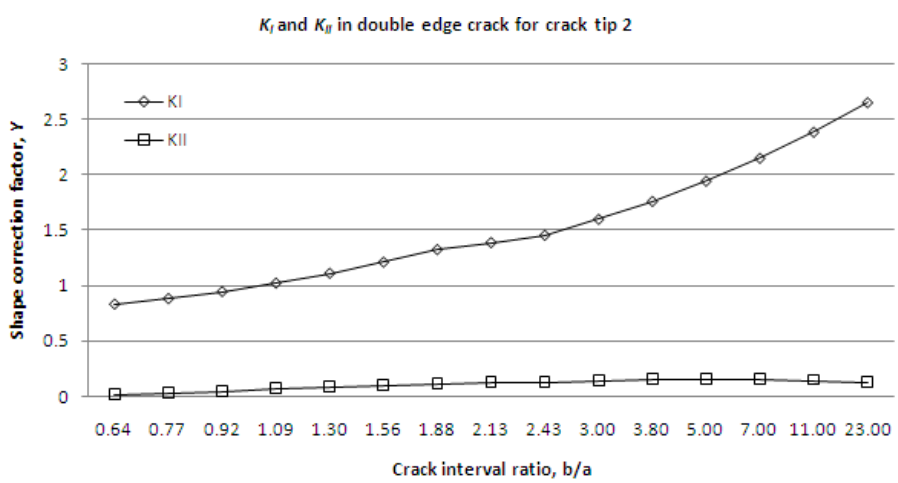

Figure-3. K_I and K_{II} in double edge crack coplanar for crack tip 2.

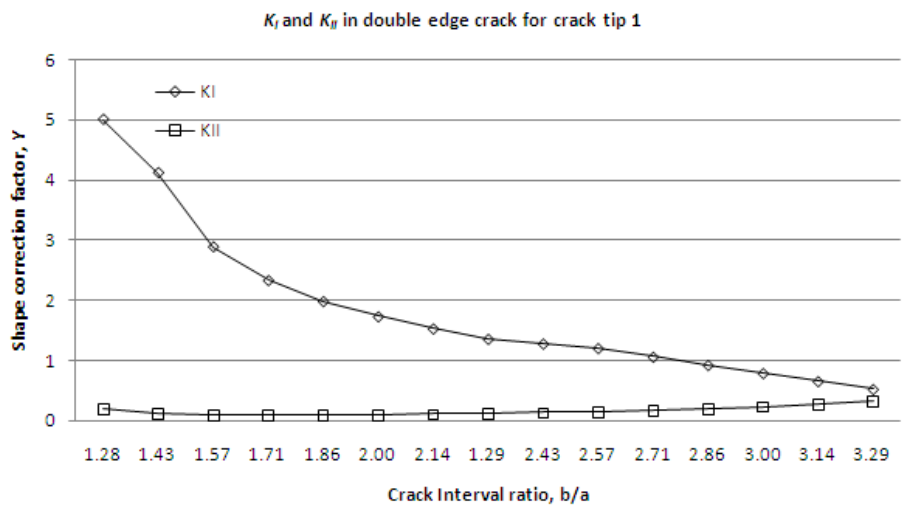

Figure-4. K_I and K_{II} in double edge coplanar crack for crack tip 1.

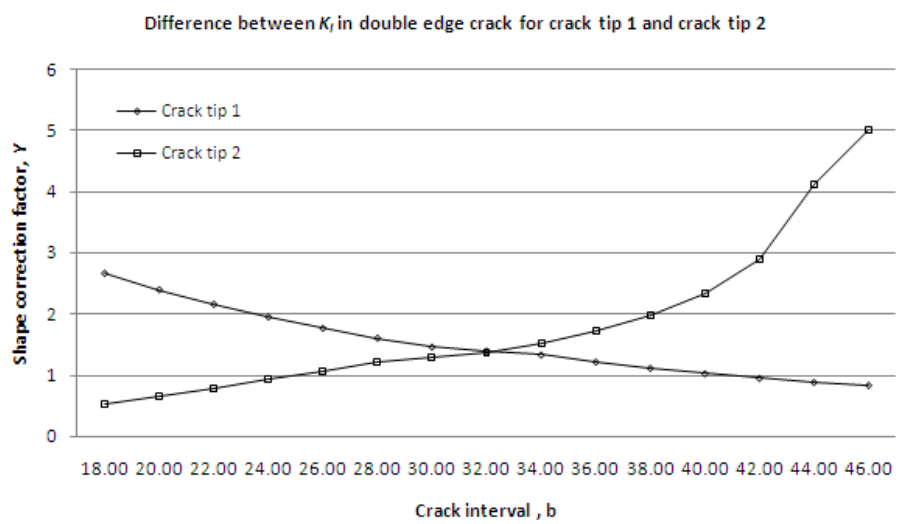

Figure-5. K_I for crack tip 1 and 2 of double edge coplanar crack.

CONCLUSIONS

Finite element modeling has proven that there are fracture behavior exist in the Mode I and Mode II stress amplication in the double edge crack where the value of stress intensity factor is found to be more significant in Mode I compared to Mode II. The value of K is differ with several value of *b*. It can be concluded that when the value of *b* increase n crack tip 1, the value of K will decrease. Contrastingly in crack tip 2, the value of K will increase when *b* escalates. This is due to the unsymmetrical of crack length in both crack tip. It also has proven that there are crack unification limit (CUL) also crack interaction limit (CIL) in the model developed. Other than that, the corresponding computational results of crack propagation have been obtained and verified using theoretical results using Brown and Srawley's (1966). It is found that the present result have good agreement with the analytical result.

ACKNOWLEDGEMENT

The authors gratefully acknowledge the financial support from short term grant given by Universiti Malaysia Perlis (V7/220807).

REFERENCES

Alia, N., Daud, R., Azman, W. Z., Faizal, A., Fadzli, M. and Aisyah, S. 2014. Numerical Simulation of Stress Amplification Induced by Crack Interaction in Human Femur Bone. Paper presented at the International Conference on Mathematics, Engineering and Industrial Applications Gurney Hotel, Penang.

Benbarek, S., Bouiadjra, B. A. B., El Mokhtar, B. M., Achour, T. and Serier, B. 2013. Numerical analysis of the crack growth path in the cement mantle of the reconstructed acetabulum. Materials Science and Engineering: C, 33(1), 543-549.

Chen, W.-P., Tang, F.-T. and Ju, C.-W. 2001. Stress distribution of the foot during mid-stance to push-off in barefoot gait: a 3-D finite element analysis. Clinical Biomechanics, 16(7), 614-620.

R. Daud, A.K. Ariffin, S. Abdullah. 2013. Validation Of Crack Interaction Limit Model For Parallel Edge Cracks Using Two-Dimensional Finite Element Analysis, International Journal of Automotive And Mechanical Engineering (IJAME), Volume 7, Pp. 993-1004.

R. Daud, M.S. Abdul Majid, M. Afendi, N.A.M. Amin, A.K. Ariffin, S. Abdullah. 2015. "Strong shielding interaction analysis using J-integral", Applied Mechanics and Materials, Vol. 695, 2015, pp. 511-515

Doblaré, M., Garcıa, J. and Gómez, M. 2004. Modelling bone tissue fracture and healing: a review. Engineering Fracture Mechanics, 71(13), 1809-1840.

Gross, B., Srawley, J. E. and Brown Jr, W. F. 1964. Stress-intensity factors for a single-edge-notch tension specimen by boundary collocation of a stress function: DTIC Document.

Huang, B., Chang, C., Wang, F., Lin, A., Tsai, Y., Huang, M. and Tseng, J. 2012. Dynamic characteristics of a hollow femur. Life Science Journal, 9(1), 723-726.

Kumar, S., Singh, I. V., Mishra, B. K. and Rabczuk, T. 2015. Modeling and simulation of kinked cracks by virtual node XFEM (Vol. 283, pp. 1425-1466): Elsevier.

Marieb, E. N. 2007. Essentials of Human Antomy and Physiology: Benjamin Cummins Press.

Olvera, D., Zimmermann, E. A. and Ritchie, R. O. 2012. Mixed-mode toughness of human cortical bone containing a longitudinal crack in far-field compression. Bone, 50(1), 331-336.

Rudraraju, S. S. 2004. Implementation of the Energy Domain Integral method in Ansys for calculation of 3D J-integral of CT-fracture specimen.

Sanati, H., Amini, A., Reshadi, F., Soltani, N., Faraji, G. and Zalnezhad, E. 2014. The stress intensity factors (SIFs) of cracked half-plane specimen in contact with semi-circular object. Theoretical and Applied Fracture Mechanics.

Shah, M., Ferracane, J. and Kruzic, J. 2009. R-curve behavior and micromechanisms of fracture in resin based dental restorative composites. Journal of the mechanical behavior of biomedical materials, 2(5), 502-511.

Wen, J.-S., Ju, W.-E., Han, T.-K., Choi, S. and Lee, K.-S. 2012. Finite element analysis of a subsurface penny-shaped crack with crack-face contact and friction under a moving compressive load. Journal of Mechanical Science and Technology, 26(9), 2719-2726. doi: 10.1007/s12206-012-0741-8

Woo, C. and Kuruppu, M. 1982. Use of finite element method for determining stress intensity factors with a conic-section simulation model of crack surface. International Journal of Fracture, 20(3), 163-178.

Xu, Z. and Li, Y. 2012. A novel method in determination of dynamic fracture toughness under mixed mode I/II impact loading. International Journal of Solids and Structures, 49(2), 366-376.

Zain, N. A. M., Daud, R., Muhamad, W. Z. A. W., Basaruddin, K. S., Baijuri, Y., Halim, S. A. A. and Mansor, N. N. 2014. Variation of stress intensity factor and crack distance length for double edge crack in human femur bone. Paper presented at the World Virtual Conference on Advanced Research in Materials and Engineering Applications.